ELSEVIER

Journal of Experimental Marine Biology and Ecology, 241 (1999) 235–261

JOURNAL OF EXPERIMENTAL MARINE BIOLOGY AND ECOLOGY

Stomatopod sniffing: the scaling of chemosensory sensillae and flicking behavior with body size

K.S. Mead[a,*], M.A.R. Koehl[a], M.J. O'Donnell[b]

[a]*Department of Integrative Biology, VLSB 3060, University of California, Berkeley, CA 94720-3140, USA*
[b]*Department of Biological Sciences, Stanford, CA 94305, USA*

Received 16 February 1999; received in revised form 15 June 1999; accepted 21 June 1999

Abstract

Many crustaceans detect odors from distant sources (such as conspecifics or prey items) by using chemosensory sensillae (aesthetascs) on their antennules. The morphology and arrangement of the aesthetascs on the antennule and the movement of the antennule through the surrounding fluid during olfactory sampling affect the flow of odorants around the sensillae and thus odorant access to receptors inside the aesthetascs. We examined fluid flow around the olfactory appendages of the stomatopod *Gonodactylus mutatus*, a crustacean with excellent olfactory capabilities, a simple arrangement of aesthetascs on their antennules, and a 10-fold range in post-metamorphic body sizes. Using morphometric and kinematic measurements, we calculated several hydrodynamic parameters including the aesthetasc Reynolds number (Re), the leakiness of the setal array, and flow rate through aesthetascs and determined how these descriptors of fluid flow changed as the animals increased in size. We found that *G. mutatus* aesthetascs operate over a range of Re where the leakiness of the aesthetasc array is very sensitive to changes in antennule speed and setal dimension. As a result, the rate of fluid flow through the array of aesthetascs varies by a factor of two during different odor-sampling motions of the antennule, and changes over 200-fold as the animals increase in size. The increases in Re, leakiness, and flow rate as the stomatopods grow suggest that stomatopods alter their odor sampling paradigm as they mature, corresponding to changes in diet, preferred habitat and behavior.

Keywords: Aesthetasc; Antennule flicking; Boundary layer; Chemosensory; Hydrodynamic; Reynolds number; Stomatopod

*Corresponding author. Tel.: +1-510-6439-048; fax: +1-510-6436-264.
E-mail address: kmead@socrates.berkeley.edu (K.S. Mead)

0022-0981/99/$ – see front matter
PII: S0022-0981(99)00087-8

1. Introduction

1.1. Chemoreception and aesthetascs

Marine crustaceans use their sense of smell to detect prey items, gain information about conspecifics, and avoid predators (Ache, 1982; Atema and Voigt, 1995; Zimmer-Faust, 1989). Most crustaceans, including lobsters, crabs, crayfish, prawns, leptostracans, anaspidans, mysids, amphipods, tanaids, isopods, ostracods, phyllopods, cumaceans and stomatopods detect odors from distant sources by using chemosensory sensillae called aesthetascs (Heimann, 1984; Hallberg et al., 1992). The aesthetascs are stiff, cuticular hair-like structures organized in arrays on the antennules (Fig. 1; Hallberg et al., 1992). Odors from food and other sources exist as patches or plumes of odorant molecules in

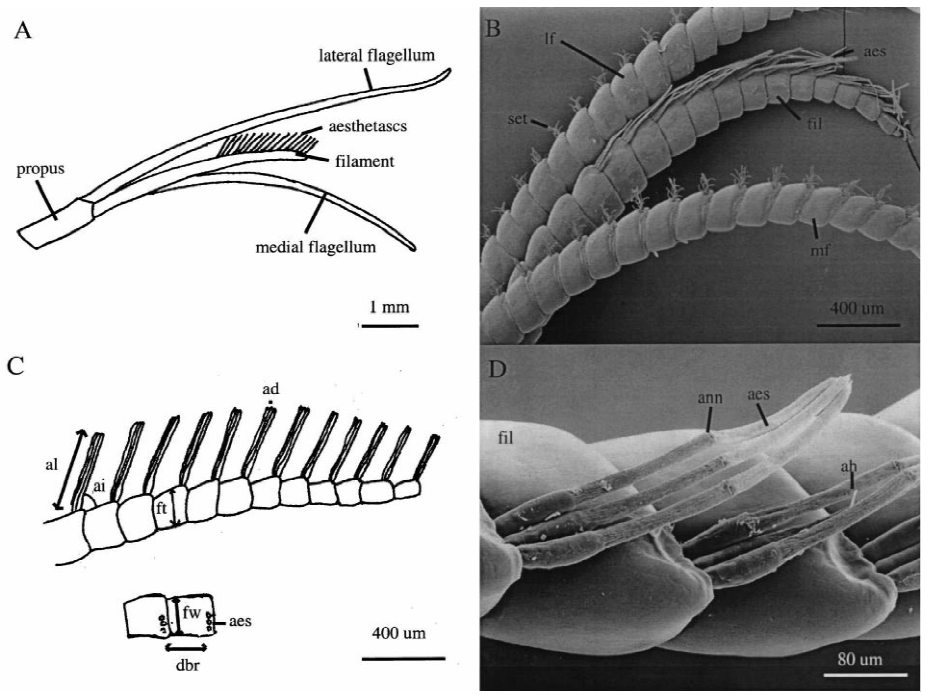

Fig. 1. Antennule and aesthetasc structure. (A) Overview of the terminal portion of a *Gonodactylus mutatus* antennule. The middle and lateral flagellae, and the aesthetasc-bearing filament of the lateral flagellum are shown. (B) SEM of an antennule from a small *G. mutatus* (rostrum–telson length 11 mm), showing the two flagellae, the filament and aesthetascs. (C) Line drawing of the distal part of the filament that branches off of the lateral flagellum. The aesthetascs are arranged in rows of three on the dorsal side of the filament, with one bundle per segment. (D) SEM of part of the aesthetasc-bearing filament of a large *G. mutatus* (rostrum–telson length 55 mm). Note the enlarged base of the aesthetascs, the ''annulus'' part way along the aesthetasc, and the narrow asymmetric hair that emerges from the back of each row of three aesthetascs. Abbreviations are as follows: ad = aesthetasc diameter, aes = aesthetasc, ah = asymmetric hair, ai = angle of insertion, al = aesthetasc length, ann = annulus, fil = antennule filament, ft = filament thickness, fw = filament width, lf = lateral flagellum, mf = medial flagellum, set = seta (non-aesthetasc).

the surrounding fluid. In order for chemoreception to work, the odor molecules must first be transported to the surface of the aesthetasc. The morphology of the aesthetascs, their arrangement on the antennule, and the movement of the antennule relative to ambient water motion affect the flow of water bearing odorants around the sensillae. This in turn affects the transport of odorants to the aesthetasc surface and hence to the chemoreceptors within the sensillae. Thus, the structure and deployment of the antennules affect the ability of the animal to identify the contents of the plume and locate its source.

1.2. Water flow affects odor molecule capture by aesthetascs

Many crustaceans sample their chemical environment by rapidly flicking their antennules through the surrounding fluid (Schmidt and Ache, 1979). Because the fluid at the interface with a solid surface, such as the surface of the antennule, does not move with respect to it (the ''no-slip condition''), a velocity gradient forms in the fluid between the antennule and the mainstream flow. Typically, the distance from the surface to the point where the velocity is 99% of the mainstream velocity is called the boundary layer (e.g., Vogel, 1994). The faster the motion of the body through the fluid (or the faster the free-stream fluid motion relative to the body), the thinner the boundary layer. The thickness of the boundary layer is very important for olfaction because it can act as a barrier to odorant access to the aesthetascs. While odorants can be very rapidly transported through the environment in currents (at speeds on the order of centimeters to meters per second), the time required to cross the boundary layer depends on the much slower process of molecular diffusion. Dimensional analysis indicates that the average time t required for a molecule to cross a boundary layer of thickness x is proportional to the square of the thickness of the boundary layer:

$$t \propto \frac{x^2}{D} \tag{1}$$

where D is the coefficient of diffusion (m^2/s). Amino acids, to which many crustaceans are responsive, typically have molecular diffusion coefficients on the order of 10^{-9} m^2/s in water. Therefore, while it might take 1 s for an amino acid to travel a meter in an ambient water current moving from a dead fish to the edge of a 100 μm boundary layer of water around a crustacean's aesthetasc, it might take 10 s on average to cross the remaining 100 μm. Furthermore, if the animal is able to reduce the boundary layer coating its aesthetasc to just 50 μm (by flicking more rapidly, for example), the time to diffuse across the boundary layer surrounding the aesthetasc decreases to 2.5 s on average. Thus the structure of the boundary layer regulates the rate of odorant access to the receptors in the aesthetascs.

To analyze the water flow past aesthetascs, we must consider the boundary layers around a number of cylindrical setae (the aesthetascs) attached to another cylinder (the antennule) when the animal is moving this appendage through the surrounding seawater during a flick. There is no simple formula for the boundary layer in this situation, but we know that the structure of the boundary layer depends on many variables, including the length and diameter of the aesthetascs, the gap between aesthetascs, their orientation on

the antennule, antennule diameter, the mainstream velocity, the density of the fluid and the dynamic viscosity of the fluid (Schlichting, 1979; Koehl, 1995).

One simple way to start understanding this complicated flow situation is to calculate the Reynolds number (Re) that describes the fluid flow around the aesthetascs during flicking. Re is a dimensionless parameter that represents the ratio of inertial to viscous forces involved in a particular flow situation:

$$\mathrm{Re} = \frac{\rho L U}{\mu} \tag{2}$$

where ρ is the density of the fluid (here the density of sea water at 25°C, 1023 kg/m^3), U is a velocity (here the antennule velocity relative to the ambient flow), L is a length unit (here the diameter of the aesthetasc), and μ is the dynamic viscosity of the fluid (here the viscosity of sea water at 25°C, $0.97 \cdot 10^{-3}$ Pa s) (Vogel, 1994). In general, $\mathrm{Re} < 1$ indicates that viscous forces are dominant and $\mathrm{Re} > 1$ suggests that inertial forces are important. For a given aesthetasc diameter, a large Re indicates that the boundary layer is thin relative to the dimensions of the object, and a small Re suggests that the boundary layer is thick relative to the body. If Re is low and boundary layers are thick relative to the diameters of the setae in an array, then little fluid may penetrate into the array.

Leakiness is a measure of fluid penetration through the gaps in an array of setae. Leakiness is defined as the ratio of the volume of fluid that flows through a gap between two cylinders in a unit of time to the volume of fluid that would have flowed through the same area in that unit of time if the cylinders had not been present (Fig. 2; Cheer and Koehl, 1987; Koehl, 1995). Leakiness can then be used to calculate the amount of fluid that flows between adjacent rows of aesthetascs per unit of time (flow rate) during different parts of the flick.

Since Reynolds number is proportional to setal (e.g., aesthetasc) diameter, and since leakiness and flow rate depend on aesthetasc diameter and spacing (Koehl, 1995), the growth of an animal might affect the performance of olfactory antennules. Furthermore, since Re, leakiness and flow rate also depend on velocity, the kinematics of antennule movements can also affect their performance. In order to examine the effects of aesthetasc size and antennule velocity on olfactory performance, we have investigated the morphological and kinematic changes in the antennules of a crustacean, the stomatopod *Gonodactylus mutatus*, as it grows from its post-settlement size to its largest adult size. We have used Re, leakiness and flow rate as performance indicators.

1.3. Stomatopod antennules and aesthetascs

We are using stomatopod antennules as a model system for examining the effect of aesthetasc morphology, aesthetasc arrangement on the antennule, and antennule movement on odorant access in marine crustaceans. Stomatopods (also known as mantis shrimp) are aggressive shrimp-like crustaceans that live in burrows in mudflats or in coral reef rubble in tropical and semi-tropical habitats. In addition to using chemical information to find food and mates, and to avoid predators (Caldwell, 1979, 1985), stomatopods depend highly on their sense of smell to identify burrows (which are critical to their feeding, reproduction and survival during molts) whose inhabitants they can

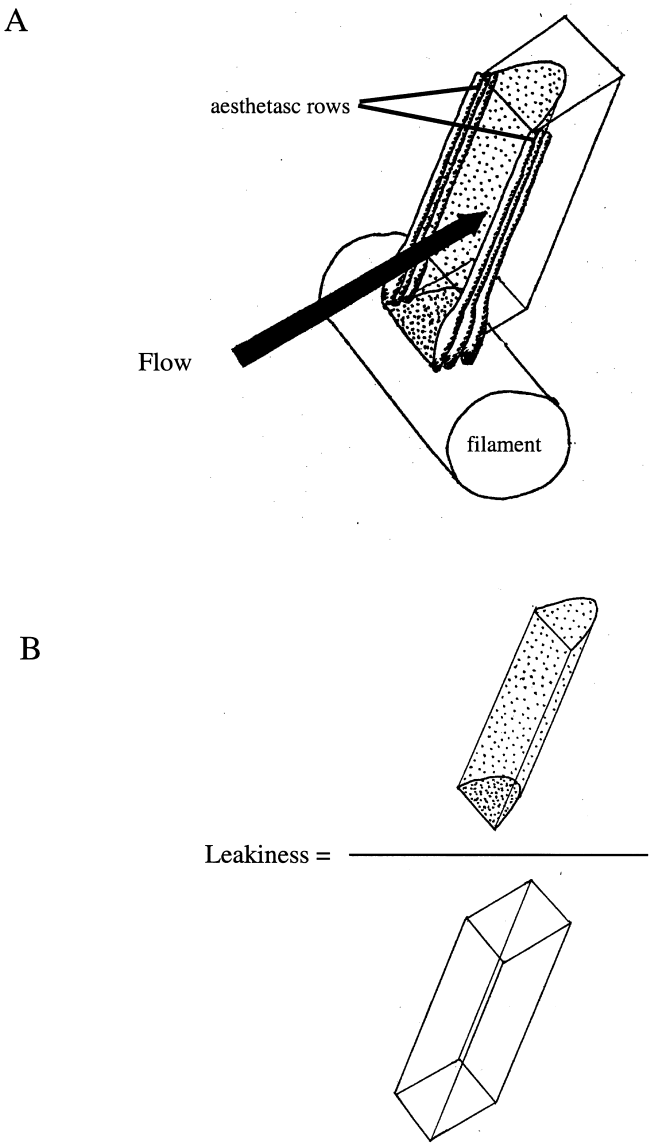

Fig. 2. Orientation of aesthetascs relative to flow and leakiness during flicking. (A) The axis of each row of aesthetascs is perpendicular to the axis of the filament and parallel to the direction of flow. (B) Leakiness is the ratio of the volume of fluid that flows between adjacent rows of aesthetascs in a unit of time (dotted volume) to the volume of fluid that would have flowed through the same area in the unit of time if the aesthetascs were not there (unfilled volume).

eject through aggressive interactions (Caldwell, 1979, 1985). Stomatopods appear to recognize by odor the individuals they have beaten and the ones by which they have been defeated in previous contests, and appear to lose this ability when their aesthetascs are removed (Caldwell, 1985).

The stomatopod antennules are preoral segmented appendages that end in two long flagellae and a robust filament that emerges from the base of the lateral flagellum and lies between the two flagellae (Fig. 1A, B). The aesthetascs are arranged in rows of three (one row per segment) on the outer portion of the dorsal side of the filament (Fig. 1C and D). In addition to the aesthetascs, there is one unobtrusive recumbent seta (of unknown function) per filament segment (Fig. 1D).

Stomatopods are excellent subjects for chemosensory studies for several reasons. (1) The simple arrangement of aesthetascs on their antennules facilitates mathematical and physical modeling of fluid flow around these sensillae. In comparison, chemosensory sensillae in crabs and lobsters are highly complex (Gleeson, 1982; Grünert and Ache, 1988). For example, the spiny lobster's olfactory organ consists of hundreds of tightly packed aesthetascs arranged in a zig-zag fashion surrounded by large curved guard hairs, asymmetric hairs and companion hairs (Gleeson et al., 1993). (2) The fact that stomatopods rely on their aesthetascs to recognize odors from specific individuals (Caldwell, 1979, 1985, 1987) indicates that aesthetasc function is important to the animal. The ease of obtaining juveniles and adults spanning an almost 10-fold range of body lengths within a species and the ease of maintaining stomatopods in the laboratory add to their experimental tractability.

In this study, we concentrate on the small, shallow subtidal tropical species of stomatopod, *Gonodactylus mutatus*. While little has been published on the life history of *G. mutatus*, work on *G. bredini*, a closely-related species, showed that post-larvae (7–12 mm rostrum–telson length) live in interstices on the surface of coral rubble and subsist on planktonic material and organic films (Caldwell et al., 1989). Larger *G. bredini* (12–15 mm body length) move into well-defined burrows in coral rubble and begin hunting small crabs, molluscs and worms during foraging forays from their burrows (Caldwell et al., 1989). During our field collections of *G. mutatus*, we noted the same size-dependent patterns in habitation and foraging. *G. mutatus* males begin breeding when they are 25–30 mm, and females when they are 35–40 mm (Caldwell, pers. comm.). The largest *G. mutatus* (mostly females) reach a maximum body length of about 55 mm (Caldwell, pers. comm.).

The purpose of this study was to determine the Reynolds number of *G. mutatus* aesthetascs, and hence the leakiness and flow rate through arrays of aesthetascs on the antennules of these stomatopods. Since water flow through an aesthetasc array (and hence odorant access) depends on the velocity of antennule motion, we studied temporal variation in velocity within a flick. Reynolds number and flow through aesthetasc arrays depend on aesthetasc size and spacing as well as on velocity, so we also investigated how the morphology and behavior of *G. mutatus* antennules scale as the animals grow. We did so for juveniles and for sexually mature males and females to determine if stomatopods of different life stages sample their chemical environment differently.

2. Materials and methods

2.1. Collection and maintenance of animals

Gonodactylus mutatus were collected from coral rubble on sand flats (water depth 0.7

to 1.5 m) in Kaneohe Bay, Oahu, HI, USA. Animals were maintained separately in small containers of artificial seawater (''Instant ocean'') at 25°C, and were fed life adult *Artemia* (brine shrimp) twice per week.

2.2. Measuring and sexing animals

Prior to each observation or antennule sampling, each animal's total body length (rostrum to telson), carapace length, rostrum length, and antennule length were measured using Mitutoyo digital calipers. Males were identified by the presence of a pair of claspers behind the third pair of walking legs. Live animals less than 13 mm long could not be reliably sexed using external characters and thus were recorded as ''juvenile''.

2.3. Scanning electron microscopy (SEM)

Excised antennules were fixed in 2% glutaraldehyde in 0.1 M sodium cacodylate buffer, pH 7.2, for 3 h to several days. The specimens were post-fixed in osmium tetroxide, washed in cacodylate buffer, and dehydrated in an alcohol series. The specimens were dried in a critical point dryer (Samdri PVT-3B, Tousimis Research Corp.), mounted on SEM stubs, and then coated with a 20 nm layer of gold (Polaron E-5400 sputter coater). Specimens were examined using a ISI-DS-130 scanning electron microscope, with a 10 kV beam. Micrographs were taken of the aesthetasc-bearing filament of each antennule from the side and from the top. Measured quantities are indicated in Fig. 2. Each parameter was measured on the micrograph using Mitutoyo digital calipers. Each measurement was repeated at the same position three times to assess measurement precision (within 0.5%). Each parameter was then measured at five replicate sites that were chosen using a grid and a random number generator. Values compared between animals of different sizes were taken from the middle of the aesthetasc tuft.

2.4. Staining

Aesthetasc permeability to small molecules in an aqueous solution was examined by exposing live stomatopods to a 0.01% solution of methylene blue in artificial seawater (32 ppt) for 1 to 60 min (after Slifer, 1960). The animals were rinsed in clean seawater for 5 min and examined under a dissecting microscope (Leica M28, 6.3–50×). This protocol indicated which portions of the aesthetasc are permeable to small molecules, a necessary requirement for olfaction. Permeable areas remained blue after rinsing. Occasionally nerve fibers inside the aesthetasc also stained blue.

2.5. Videomicrography

Sixty *G. mutatus* ranging in size from 7.6 mm to 55 mm were videotaped at 60 frames per second through a dissecting scope (Leica M28, 6.3–50×) using an Optronics Engineering LE 470 camera and a Sony SVO-5800 VCR. In early investigations, the animals were free to move around in a small dish of sea water; in later sessions, stomatopods were immobilized by placing them side, ventral, or dorsal surface up and

covering their carapace and telson with dental wax. Flagella length, width and thickness, filament length, width and thickness, distance between aesthetasc rows, angle of aesthetasc insertion, and aesthetasc length were measured from single frames on a VCR monitor using Mitutoyo digital calipers and a protractor.

2.6. High speed video and digitization

To investigate antennule kinematics, 13 animals ranging in length from 8.4 mm to 53 mm were placed one at a time into a glass or plexiglass aquarium with an artificial burrow. The glass aquarium used for larger animals measured 17.5 cm (height, H)×12 cm (width, W)×23 cm (length, L). The artificial burrow used for large animals consisted of a plastic vial with a hole (13 mm diameter) in its lid, which was screwed into a partition at a distance of 4 cm from the front wall of the aquarium. Mirrors placed at an angle of 45° from the burrow made three-dimensional (3D) video analysis possible, although subsequent calculations showed that two-dimensional (2D) video analysis was sufficient when flicks were chosen whose movement was within the focal plane (see Results). Smaller animals were filmed in a plexiglass aquarium 6 cm (W)×6 cm (H)×8 cm (L). A divider with one of three interchangeable burrows (pipette tips of various sizes) was placed 2 cm from the front wall. Burrow sizes in the small aquarium were 2.3 mm, 5.0 mm, or 6.25 mm in diameter. All animals were given one to two days before they were videotaped to acclimate to the tank and to find the burrow. After being deprived of food for a day, the stomatopod was videotaped at 250 frames per second using a high-speed video system (NAC color high-speed video, hsv-1000 fps). Fiber optics lamps (Cole Parmer 9741-50) were used as a light source to minimize heating the aquarium. The water in the aquarium was kept at 25°C. The temperature of the water in the aquarium was monitored frequently since any increase in temperature would affect flicking both by increasing the animal's metabolic rate and by decreasing the viscosity of the sea water. Brine shrimp odorant was prepared by placing a high concentration of living adult *Artemia* in artificial seawater for one to two days, and then pouring off the liquid. When we injected 2–5 ml brine shrimp odor into the top portion of the tank out of a stomatopod's field of view, the stomatopod began moving its antennules rapidly in a stereotypic flicking behavior called ''antennulation'' (Caldwell, 1979). These movements were captured on video, and analyzed using image digitization software from Peak Motus Performance Technologies (version 2.0). The positions of the base of the antennule, the distal end of the propus, the tips of the flagellae, and the tip of the aesthetasc-bearing filament were recorded 250 times per second. 10 flicks were digitized per animal. Digitized data files were scaled (from pixels to mm) within Peak Motus and exported to Microsoft Excel 5.0 spreadsheets. We calculated linear and angular filament tip displacement, and maximum and mean antennule velocities tangential to the arc inscribed by the filament tip of the antennule for both strokes of the flick. We also calculated the maximum and mean angular velocities for the two strokes of the flick, and the position of the aesthetasc-bearing antennule filament relative to the base of the antennule at the beginning and end of each flick. In each case, the values of these parameters from ten flicks were used to calculate means that were then used in further analyses.

2.7. Leakiness and flow rate calculations.

Leakiness is the ratio of the volume of fluid that flows between adjacent rows of aesthetascs in a unit of time to the volume of fluid that would have flowed through the same area in the unit of time if the aesthetascs were not there (Fig. 2). We made estimates of the leakiness of the gaps between rows of aesthetascs by assuming that a row of three closely-spaced aesthetascs oriented with the long axis of the row perpendicular to the flow functioned as a single cylinder. We used aesthetasc diameter and the mean tangential velocity of the aesthetasc-bearing filament tip to calculate Reynolds number (Eq. (2)). We used the distance between aesthetascs as the gap width and aesthetasc diameter as the cylinder diameter to calculate the gap:diameter ratio (G/D). These values of Re and G/D were used to read estimates of leakiness on the graphs in Figs. 3 and 10 in Koehl (1995). The leakiness values that we used for $\mathrm{Re}<0.5$ were calculated from the mathematical model generated by Cheer and Koehl (1987), while leakiness values for higher Res were determined from tow-tank experiments with comb-like physical models by Hansen and Tiselius (1992). When necessary, we interpolated values between the points plotted in Figs. 3 and 10 in Koehl (1995) by making the simplifying assumption that leakiness increases linearly with G/D and with Re in the narrow range between points. We calculated the rate of fluid flow (volume/time) between two adjacent rows of aesthetascs to be:

$$\text{flow rate} = L_a L_g V \times \text{leakiness} \times \sin \alpha \tag{3}$$

where L_a is the aesthetasc length, L_g is the distance between adjacent rows of aesthetascs, V is tangential velocity of the filament tip during the portion of the flick under study, and α is the angle at which the aesthetascs are inserted into the antennule filament (Fig. 1). This calculation makes the assumption that leakiness and flow rate are independent of position along the aesthetasc. Leakiness should be lower near the bases of the aesthetascs due to the boundary layer along the filament surface and should be higher near the filament tips (Best, Loudon and Koehl, unpublished data), so our calculation of flow rate based on mid-aesthetasc leakiness is just a rough estimate. We also calculated the volume/time of fluid processed by an entire array of aesthetascs by calculating the flow rate between each pair of adjacent aesthetasc rows. Since the antennule filament in *G. mutatus* is rigid, we assumed that the velocity with which an aesthetasc moves through the fluid is a linear function of the aesthetasc's position on the antennule, and adjusted the velocity and leakiness for each pair of adjacent aesthetasc rows accordingly.

2.8. Analysis and statistics

We plotted various antennule and aesthetasc morphological and kinematic parameters as a function of stomatopod rostrum–telson length. We then calculated Standard Model I linear regressions examining the scaling of these elements with body size using the statistics package in Microsoft Excel 5.0. Because standard least-squares linear regressions of allometric relationships with a low r^2 can lead to an underestimate of the slope

(LaBarbera, 1989), we estimated the effect of the error of the independent variable on the slope. We used the reliability ratio κ (where $\kappa = r$, and r is the correlation between repeated measurements of stomatopod rostrum–telson length; Fuller, 1987) to estimate the measurement error in our independent variable (Johnson and Koehl, 1994). We then corrected the slope by multiplying the slope by $1/\kappa$. Minimum significant differences (used to determine if regression slopes differed significantly from each other) were calculated using the Tukey–Kramer method (Sokal and Rohlf, 1995).

2.9. Flicking frequency

Segments of high-speed video showing rapid flicking movements were digitized and analyzed as above. Stomatopods intersperse bouts of intensive flicking with periods of quiescence of varying lengths. Flicking frequencies within bouts of at least four flicks were calculated. Five flicking frequencies were calculated per specimen.

3. Results

3.1. Stomatopod rostrum–telson length

Our measurements of stomatopod rostrum–telson lengths generated a reliability ratio κ of 0.99.

3.2. External aesthetasc morphology

G. mutatus aesthetascs are thin cuticularized structures that are enlarged at the base, and have an annulus about 60% of the distance along the aesthetasc from the base (Fig. 1D). As animals grow from 8 to 55 mm rostrum–telson length, the number of rows of aesthetascs increases from 3 to 18, and aesthetasc length increases from 150 to 550 μm (Fig. 3A and D; Table 1). The length and diameter of the filament on which the aesthetascs are borne also increases with body size (Fig. 3B and C; Table 1). In contrast, the angle at which the aesthetascs are inserted into the filament and the distance between the rows of aesthetascs do not vary with body size (Figs. 3E and F, Table 1).

Associated with each row of aesthetascs is a small seta (4 to 5 μm diameter) of unknown function, possibly analogous to the asymmetric mechanosensory sensillae of the spiny lobster *Panulirus argus* (Gleeson et al., 1993). The medial and lateral flagellae of a stomatopod antennule also bear setae (that are not aesthetascs); these are 60 to 100 μm long and 4 to 5 μm in diameter.

Measurements from scanning electron micrographs indicate that aesthetasc diameter and the diameter of the presumptive asymmetric sensillae increase with body size (Fig. 4A and B; Table 1), whereas the diameters of the setae on the medial and lateral flagellae do not increase with body size (Fig. 4C; Table 1).

While aesthetascs show sexual dimorphism in some decapods, cladocerans, mysids, copepods, anaspids, amphipods, tanaids, and cumaceans (Hallberg et al., 1992), there is no significant morphological difference between the antennules or aesthetascs of male

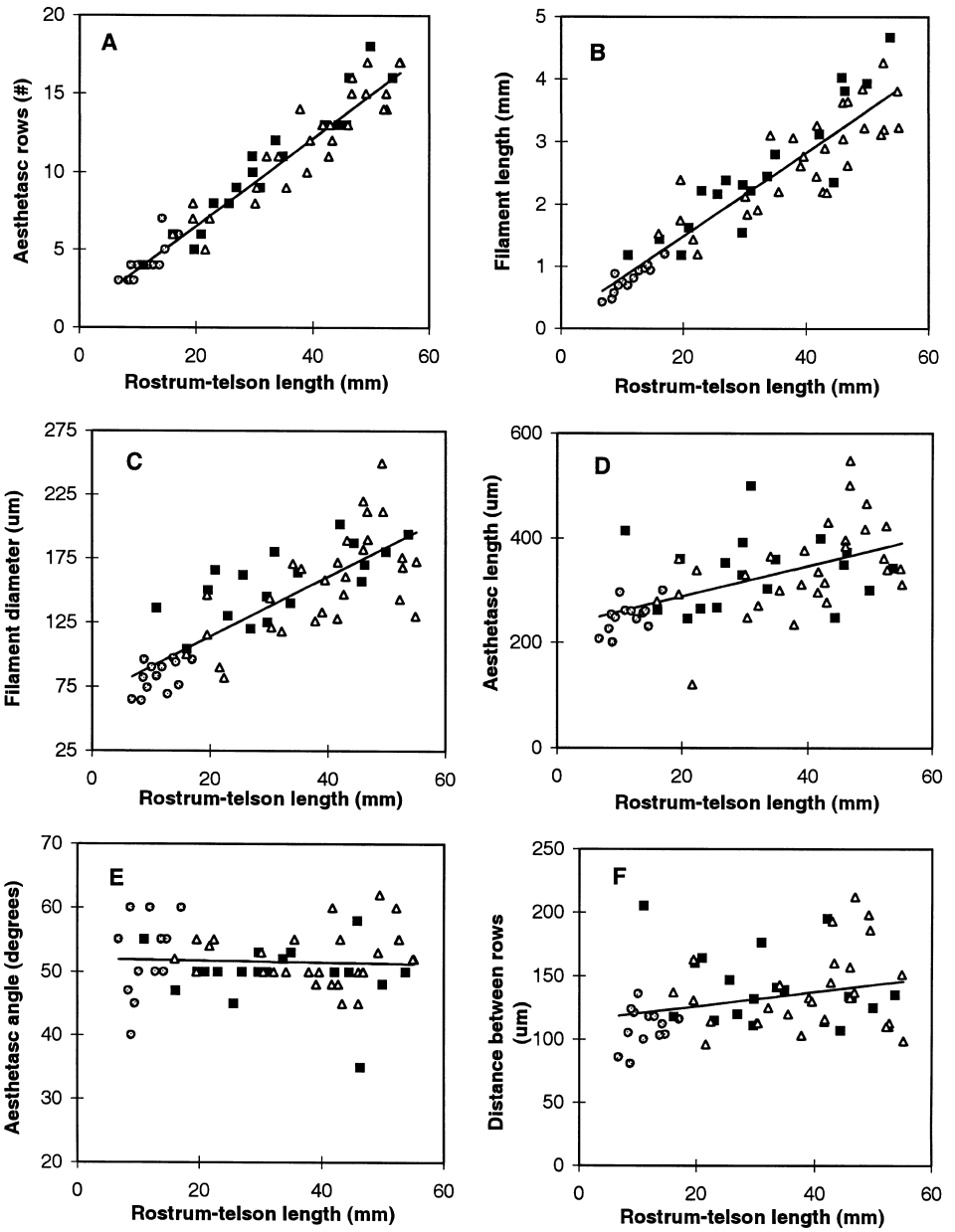

Fig. 3. Scaling of structural elements with body size. Data are means and standard errors from 61 specimens studied through dissecting scope. Solid squares are males, open triangles are females, and grey circles are juveniles. Linear regressions shown are based on all 61 specimens. (A) Aesthetasc bundles. (B) Filament length. (C) Filament diameter. (D) Aesthetasc length. (E) Aesthetasc angle. (F) Distance between rows of aesthetascs.

Table 1
Scaling of structural features of the antennule filament bearing the aesthetascs in the stomatopod *Gonodactylus mutatus*[a]

Category	Sex	R^2	Slope	y Intercept	P slope = 0	95% confidence	MSD
No. of aesthetasc rows	Male	0.93	0.31±0.02	0.36±0.76	<0.000001	0.26–36	0.07
per mm rostrum–telson length	Female	0.86	0.28±0.02	1.0±0.89	<0.000001	0.23–32	0.06
Aesthetasc filament length (μm)	Male	0.84	76±8	56±291	<0.000001	58–94	24
per mm rostrum–telson length	Female	0.67	56±8	497±308	<0.000001	41–72	23
Filament diameter (μm)	Male	0.49	1.54±0.39	106±14	0.001	0.71–20.4	1.16
per mm rostrum–telson length	Female	0.43	2.28±0.51	66±21	0.0001	1.25–3.32	1.47
Aesthetasc length (μm)	Male	0.003	0.28±1.4	328±47	0.84	−2.6–3.2	4.04
per mm rostrum–telson length	Female	0.26	3.8±1.2	195±50	0.005	1.25–6.3	3.55
Aesthetasc angle (degrees)	Male	0.03	−0.06	52±3	0.52	−0.26–0.14	0.28
per mm rostrum–telson length	Female	0.006	0.028±0.069	51±3	0.68	−0.11–0.17	0.20
Distance between aesthetasc rows (μm)	Male	0.08	−0.63±0.55	163±19	0.27	−1.8–0.5	1.63
per mm rostrum–telson length	Female	0.04	0.52±0.50	116±21	0.31	−0.5–1.6	1.47
Aesthetasc diameter (μm) per mm rostrum–telson length	Both	0.7	0.197±0.049	7.8±2	0.005	0.08–0.314	
Asymmetric sensillum diameter (μm) per mm rostrum–telson length	Both	0.9	0.07±0.01	1.5±0.4	0.001	0.044–0.099	
Seta diameter on lateral, medial flagellae (μm) per mm rostrum–telson length	Both	0.04	0.017±0.032	4.0±1.3	0.65	0.92–7.02	

[a] Model I linear regressions with slopes corrected for error in measurement of the total body length ($\kappa = 0.99$). For categories 1–6, $n = 60$ (18 males, 29 females, 13 juveniles) and $n = 9$ for categories 7–9 (two males, three females, four juveniles). MSD = Minimum significant difference.

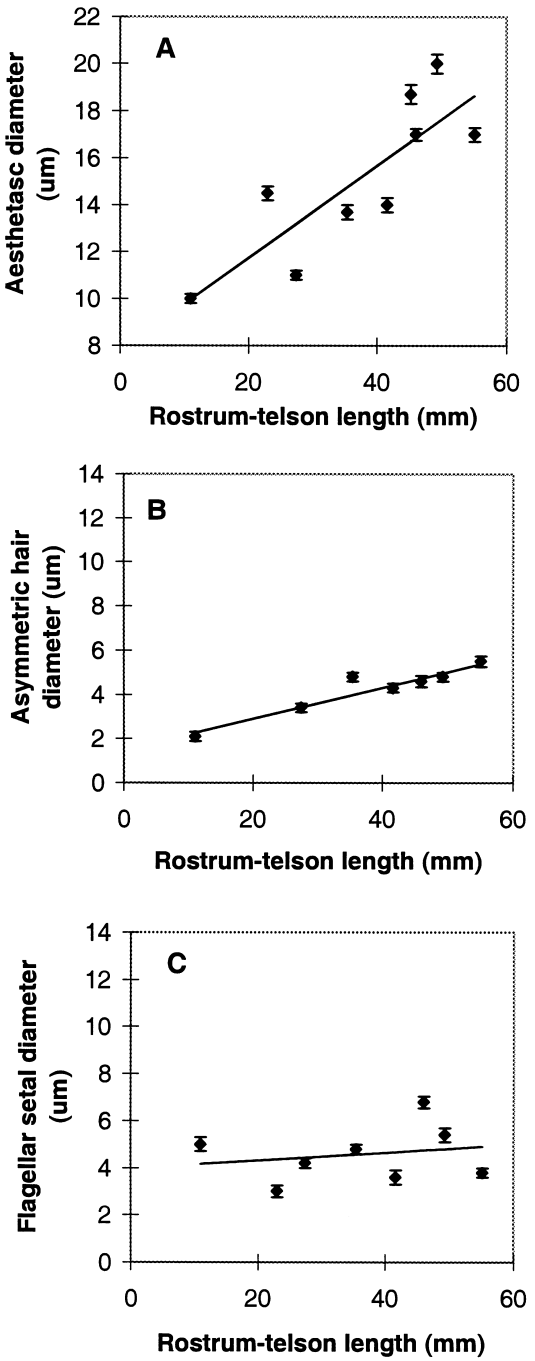

Fig. 4. Scaling of structural elements with body size. Data are means and standard errors for nine animals examined in SEM. (A) Aesthetasc diameter. (B) Diameter of asymmetric sensillae. (C) Diameter of setae on medial and lateral flagellae.

and female *G. mutatus*. The slopes of linear regressions of all structural parameters tested (number of aesthetasc rows, filament length, filament diameter, aesthetasc length, aesthetasc angle and distance between rows of aesthetascs) as a function of total body length show no significant differences between males and females (Table 1).

3.3. Internal aesthetasc and filament morphology

Dye studies showed that the aesthetasc cuticle is readily permeable to methylene blue after only a few seconds of exposure to the dye. This suggests that the cuticle is permeable to other small molecules, such as amino acids. Cuticle permeability is a minimum requirement for identifying the sensillae as aesthetascs, since the odorants need to be able to penetrate the cuticle in order to gain access to chemoreceptors on the surface of sensory nerves inside the aesthetasc. The cuticle appeared to be permeable to dye along the entire length of the aesthetasc. After rinsing, the dye was darkest in small (20–30 μm diameter) cord-like structures inside the filament, tentatively identified as nerve bundles.

3.4. Kinematics

Stomatopod investigatory antennulation consists of a series of small flicks of one or both antennules. Antennulation usually consists of several rapid flicks along a single axis, followed by a pause as the stomatopod repositions its antennules, and then begins to flick again (Fig. 5A). The right and left antennules can flick in synchrony or independently (Fig. 5B). Each flick starts with a rapid, outward lateral movement followed by a slower return medial movement (Fig. 5C). The outward movement lasts for 33 ± 2 ms and the return motion lasts for 43 ± 3 ms regardless of body size. Fig. 6 shows that seen from the front, flicks can start at almost any angle.

As long as we chose flicks whose entire motion was within the focal plane of the camera, 2D and 3D analysis gave trajectories and velocities that agreed to within 5%. 3D analysis confirmed that the flicks that we chose were representative of the entire population of flicks in terms of duration, tangential velocity, angular velocity and flicking frequency.

In all flicks the mean tangential velocity of the aesthetasc-bearing filament is 1.90 (S.E. = 0.03, $n = 130$) times as large during the lateral part of the flick as it is during the medial motion of the flick. The maximum tangential filament velocity is 1.88 (S.E. = 0.02, $n = 130$) times larger than the mean lateral tangential velocity (Fig. 7A). Similarly, maximum angular velocities are on average 2.29 (S.E. = 0.04, $n = 130$) times greater than lateral angular velocities, which are 2.08 (S.E. = 0.02, $n = 130$) times greater than medial angular velocities (Fig. 7B). Tangential filament velocities (maximum, lateral and medial) do not appear to change with body size when animals are small (rostrum–telson length 8–25 mm). Once the animals have a rostrum–telson length greater than 25 mm, tangential filament velocities increase three to four-fold with body size (Fig. 7A). Lateral velocities increase faster with body size in males than in females (Table 2). Angular filament velocities do not change significantly with body size (Fig. 7B, Table 2).

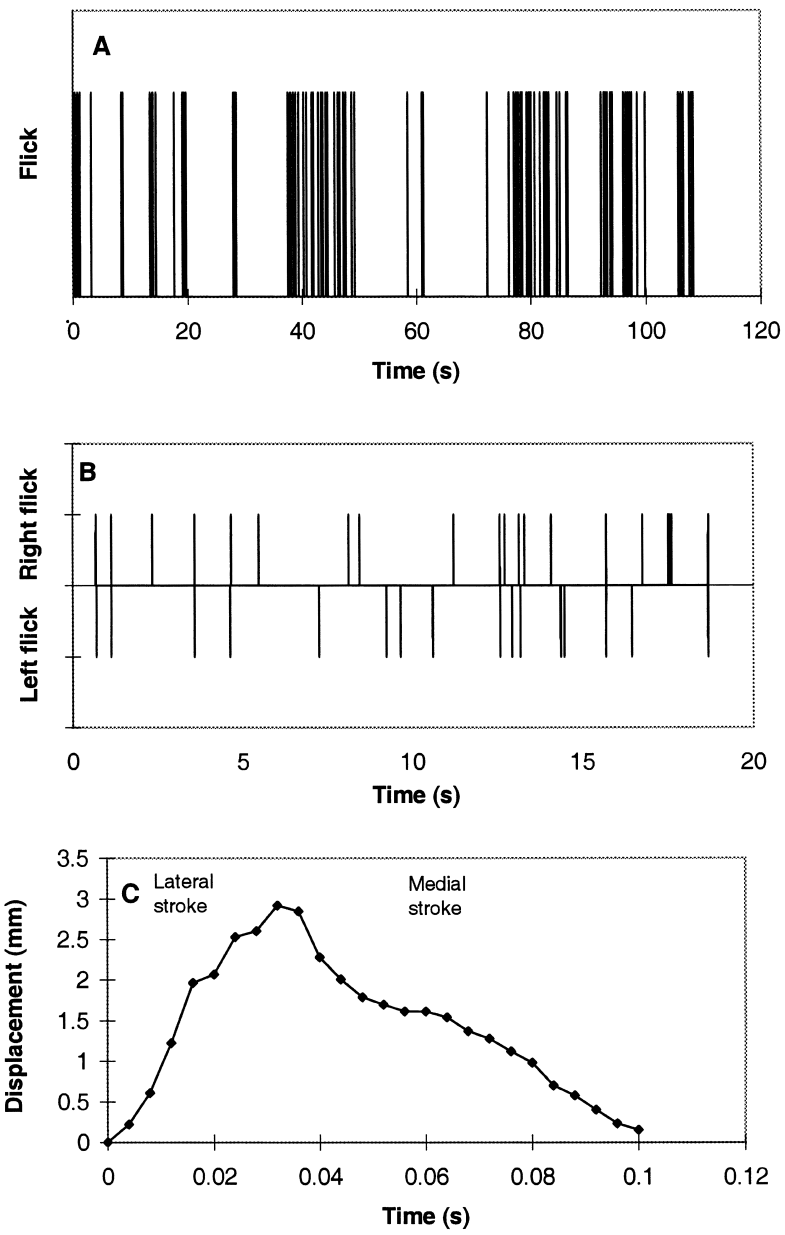

Fig. 5. Flick parameters for a 52 mm (rostrum–telson length) stomatopod. (A) Stomatopods antennulate in bursts of flicks. (B) Right and left antennules flick in synchrony or independently. (C) Profile of a typical flick.

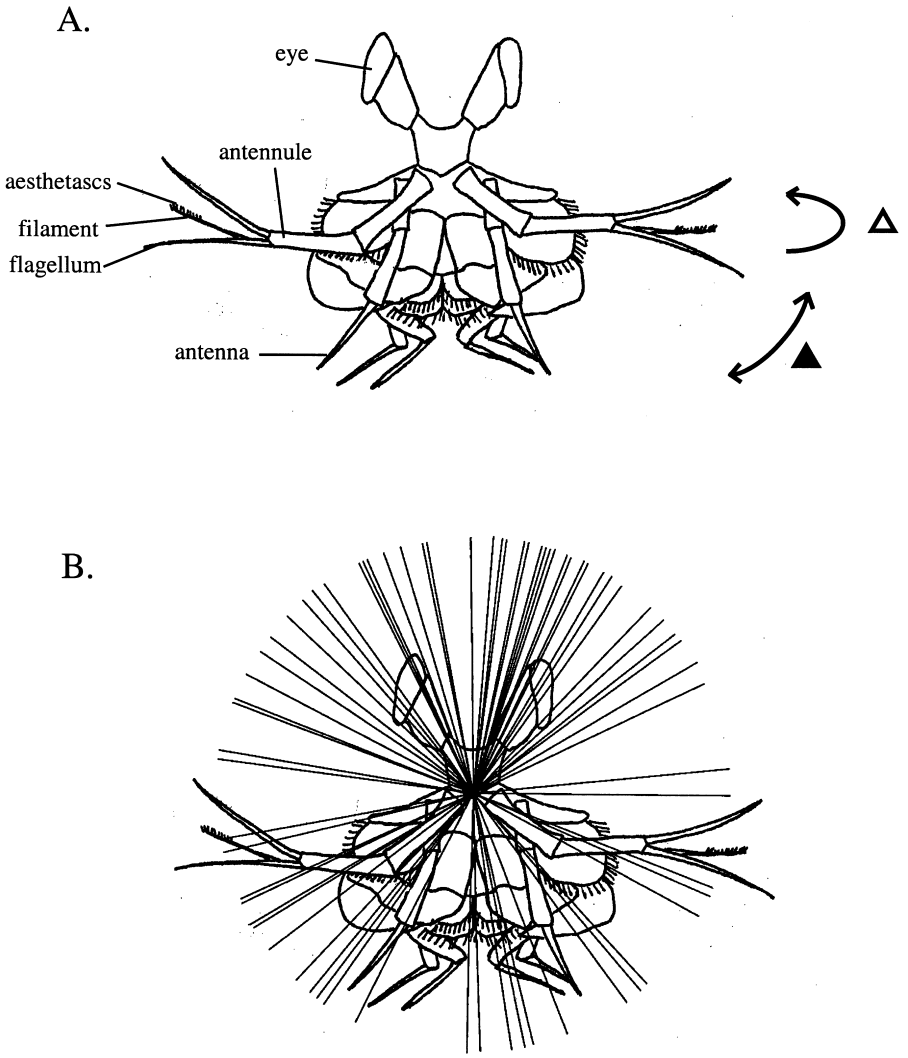

Fig. 6. Orientation of olfactory flicks. (A) Front view of stomatopod showing position and direction of flicks relative to rostrum. During a flick, the antennule can move in and out of the plane of the figure (open triangle), in a dorso–ventral direction (solid triangle), or in a combination of the two axes. The outward or dorsal movement is termed the lateral portion of the flick, and the inward or ventral motion is called the medial part of the flick. (B) Flick orientation relative to rostrum. Starting position of 108 digitized flicks relative to rostrum. From the observer's point of view facing the stomatopod, all flicks starting on the left moved in a clockwise direction and then returned to their initial position. Conversely, all flicks starting on the right moved in a counter-clockwise direction before returning to their initial position.

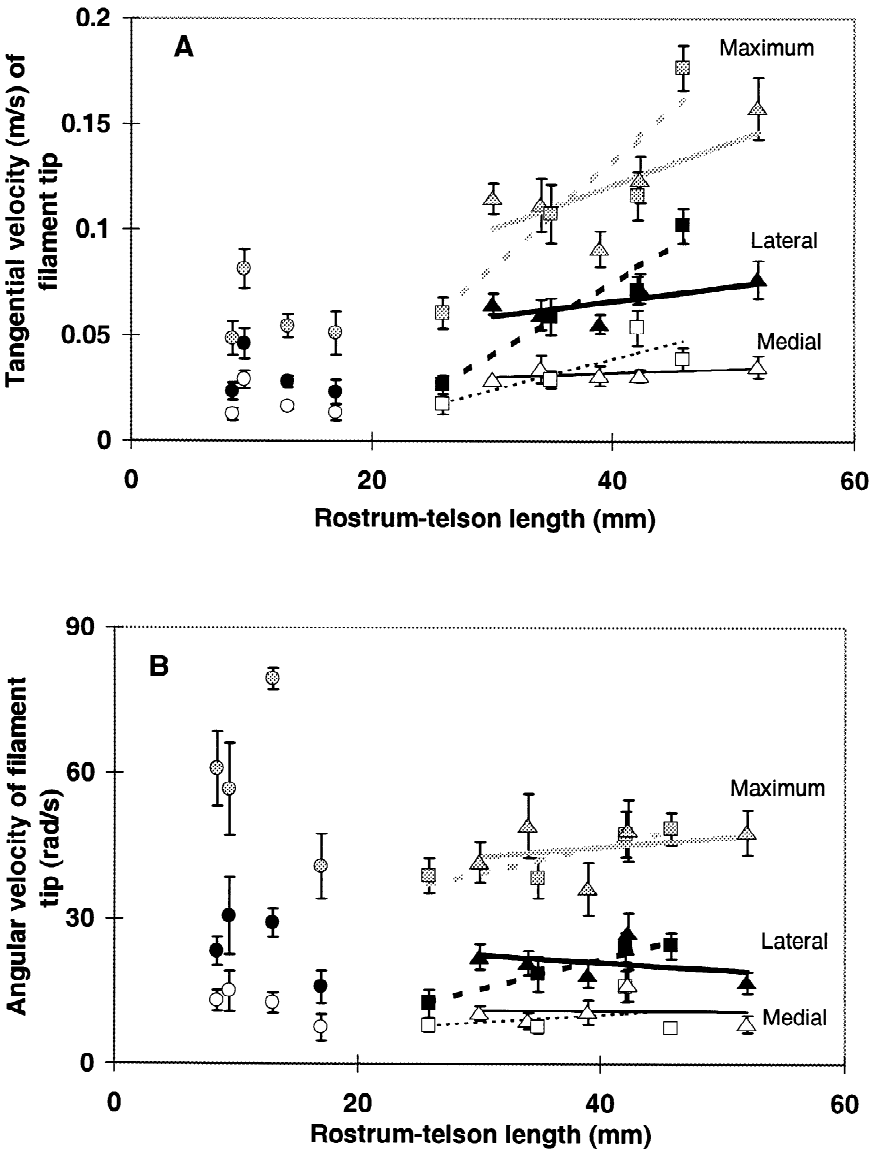

Fig. 7. Scaling of velocity of aesthetasc tip with body size. Data are means and standard errors from high speed video measurements of 13 specimens. Ten flicks were digitized per individual. (A) Maximum tangential velocity (grey symbols), mean tangential velocity during the lateral motion of the flick (filled symbols), mean tangential velocity during the medial motion of the flick (open symbols). (B) Maximum angular velocity (grey symbols), mean angular velocity during the outward motion of flick (filled symbols), mean angular velocity during the return motion of flick (open symbols). In both A and B, triangles represent females, squares indicate males, and circles show juveniles. Solid lines show linear regressions for males, dashed lines show linear regressions for females.

Table 2
Scaling of the filament tangential velocity, Reynolds number describing flow around the aesthetascs, leakiness, flow rate and flicking frequency with body size[a]

Category	Sex	R^2	Slope	y Intercept	P slope = 0	95% confidence intervals	MSD
Filament maximum tangential velocity	Male	0.87	5.1±1.4	−73±54	0.070	−1–11.1	6.3
(mm/s per mm rostrum–telson length)	Female	0.52	2.1±1.2	37±47	0.17	−1.6–5.8	4.6
Filament mean tangential velocity	Male	0.94	3.4±0.6	−64±0.23	0.029	0.85–6.1	2.7
during the lateral flick stroke	Female	0.47	0.72±0.44	38±18	0.20	−0.7–2.1	1.7
(mm/s per mm rostrum–telson length)							
Filament mean tangential velocity	Male	0.70	1.5±0.7	−21±26	0.16	−1.5–4.4	3.2
during the medial flick stroke	Female	0.41	0.19±0.13	25±5.4	0.249	−0.2–0.61	0.51
(mm/s per mm rostrum–telson length)							
Filament maximum angular velocity	Male	0.78	0.55±0.20	23±8	0.11	−10–56	0.9
(degrees/s per mm rostrum–telson length)	Female	0.09	0.20±0.36	37±15	0.62	−10–83	1.41
Filament mean angular velocity	Male	0.98	0.64±0.07	−4±3	0.01	−15–7	0.3
during the lateral part of the stroke	Female	0.11	−0.15±0.26	27±10	0.58	−5–60	1.02
(degrees/s per mm rostrum–telson length)							
Filament mean angular velocity	Male	0.11	0.16±0.32	4±12	0.67	−49–56	1.44
during the lateral part of the stroke	Female	0.001	−0.01±0.22	11±9	0.97	−17–39	0.86
(degrees/s per mm rostrum–telson length)							

Reynolds number describing the lateral flick stroke	Male	0.94	0.067±0.012	−1.4±0.47	0.03	0.016–0.117	0.054
(Re per mm rostrum–telson length)	Female	0.81	0.027±0.007	0.029±0.3	0.036	0.003–0.05	0.027
Reynolds number describing the medial flick stroke	Male	0.77	0.03±0.01	−0.53±0.43	0.12	−0.019–0.79	0.045
(Re per mm rostrum–telson length)	Female	0.88	0.01±0.002	0.14±0.085	0.019	0.003–0.0	0.0079
Mean leakiness during the lateral flick stroke	Male	0.65	0.013±0.007	0.25±0.26	0.19	−0.016–0.043	0.032
(leakiness per mm rostrum–telson length)	Female	0.01	−0.001±0.004	0.79±0.15	0.85	−0.013–0.011	0.016
Mean leakiness during the medial flick stroke	Male	0.62	0.016±0.009	0.02±0.009	0.21	−0.020–0.056	0.041
(leakiness per mm rostrum–telson length)	Female	0.08	0.003±0.005	0.51±0.2	0.64	−0.013–0.018	0.020
Mean flow rate during outward part of flick	Male	0.93	0.17±0.03	−4.03±1.26	0.036	0.028–0.31	0.14
(mm^3/s per mm rostrum–telson length)	Female	0.14	0.031±0.044	0.69±1.77	0.53	−0.11–0.17	0.17
Mean flow rate during return part of flick	Male	0.44	0.085±0.067	−1.96±2.55	0.33	−0.2–0.37	0.30
(mm^3/s per mm rostrum–telson length)	Female	0.11	0.01±0.02	0.36±0.66	0.57	−0.04–0.06	0.08
Maximum flicking frequency	Male	0.87	−0.04±0.02	8.6±0.63	0.23	−0.24–0.16	0.09
(flicks/s per mm rostrum–telson length)	Female	0.87	0.06±0.03	4.0±1.1	0.16	−0.06–0.18	0.12

[a] Model I linear regressions with slopes corrected for error in measurement of the total body length ($\kappa = 0.99$). $n = 13$ (four males, five females, two juveniles), except for category 9 ($n = 11$; three males, four females, two juveniles). MSD = Minimum significant difference.

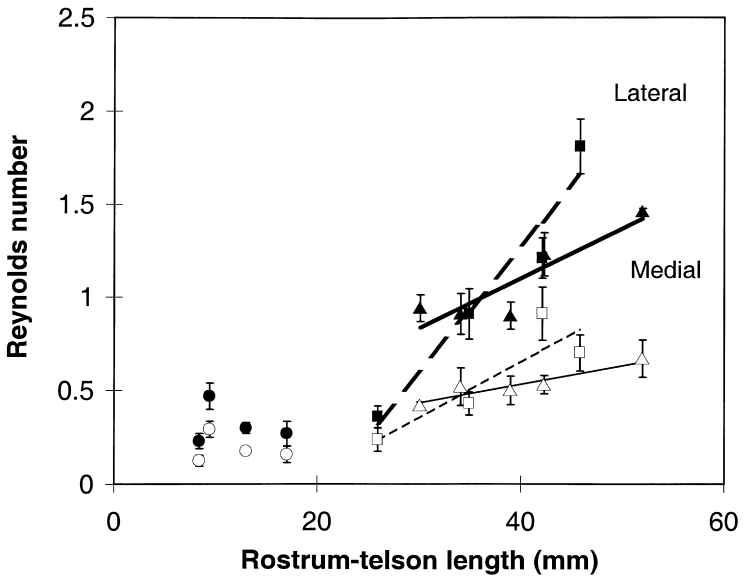

Fig. 8. Scaling of Reynolds number with body size. Length element = aesthetasc diameter. Data are means and standard errors from calculated Reynolds numbers for 13 specimens. Lateral motion of flick (filled symbols), medial motion of flick (open symbols). Triangles indicate females and squares show males. Solid lines show linear regressions for males, dashed lines show linear regressions for females.

3.5. Reynolds number

Fig. 8 shows how the Reynolds number (Re) varies with body size. Re is 1.91 (S.E. = 0.03, $n = 130$) times greater during the lateral (outward) motion of the flick than during the medial (return) motion. The combined increase in aesthetasc size and in antennule tangential velocity causes the Re of the lateral movement of the antennule ($Re_{lateral}$) to increase from 0.2 to 1.8 and Re_{medial} to increase from 0.1 to 0.9 as the animals increase in size from 8 mm to 52 mm rostrum–telson length (Fig. 8). There is no statistically significant difference between the Reynolds numbers of male and female *G. mutatus* (Table 2).

3.6. Leakiness

Fig. 9 shows the mean leakiness during the lateral and medial parts of the flick. Note that there is a general increase in leakiness with body size, and that an average of 1.23 (S.E. = 0.01, $n = 130$) times more fluid leaks through the aesthetascs during the outward part of the flick than during the return part of the flick. There is no statistically significant difference in leakiness between male and female stomatopods (Table 2).

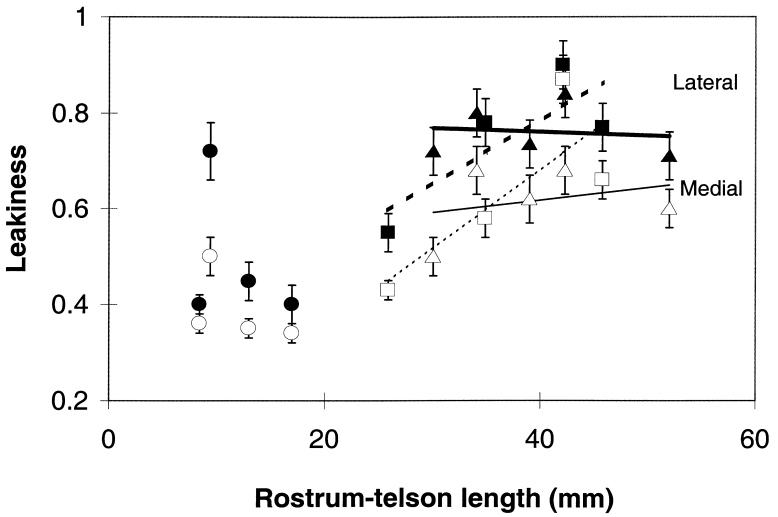

Fig. 9. Calculated leakiness during flicking. Data are means and standard errors of the leakiness between adjacent aesthetasc rows of 13 specimens. Lateral motion of flick (filled symbols), medial motion of flick (open symbols). Triangles indicate females and squares show males. Solid lines show linear regressions for males, dashed lines show linear regressions for females.

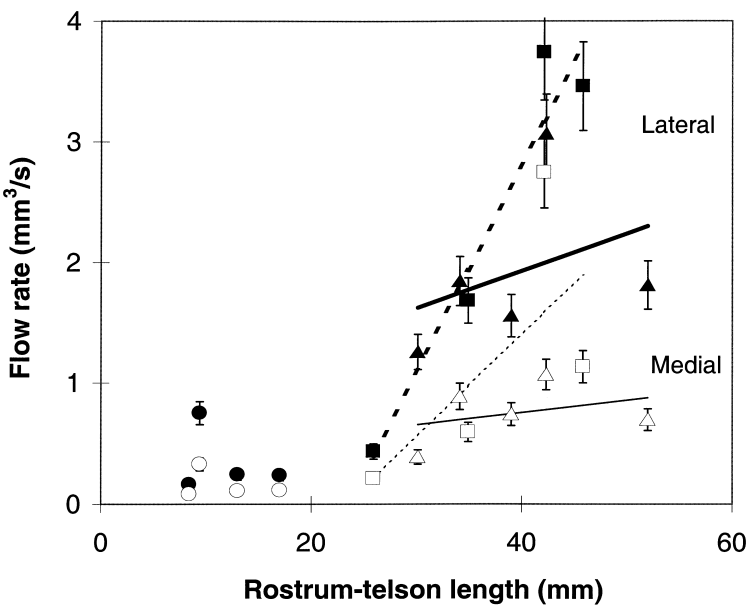

Fig. 10. Flow rate between adjacent rows of aesthetascs. Data are means and standard errors of the flow rate between two adjacent aesthetasc rows near the tip of the aesthetasc-bearing filament. $n = 13$. Lateral motion of flick (filled symbols), medial motion of flick (open symbols). Triangles indicate females and squares show males. Solid lines show linear regressions for males, dashed lines show linear regressions for females.

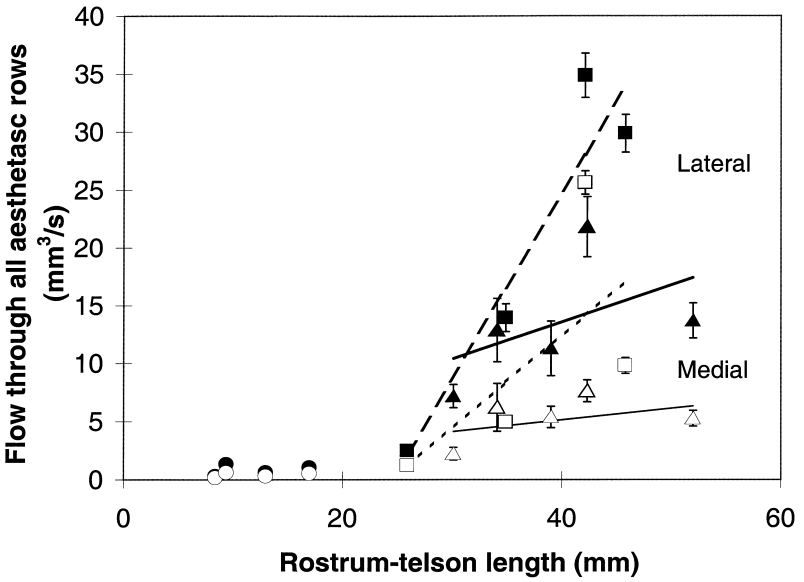

Fig. 11. Flow rate between all aesthetasc rows on an antennule. Data are means and standard errors of the flow rate between all the aesthetasc rows on the aesthetasc-bearing filament. $n=13$. Lateral motion of flick (filled symbols), medial motion of flick (open symbols). Triangles indicate females and squares show males. Solid lines show linear regressions for males, dashed lines show linear regressions for females.

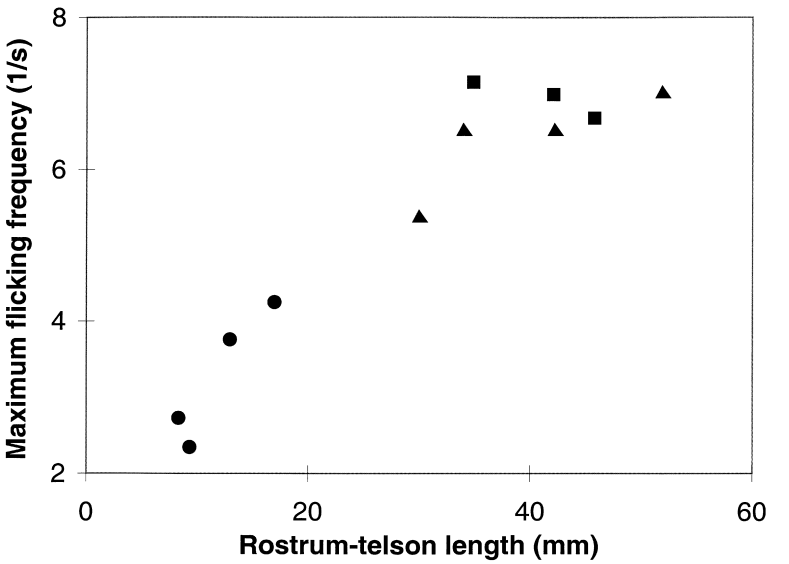

Fig. 12. Maximum flicking frequency. Data are maximum flicking frequencies of bouts lasting for at least five flicks. $n=13$. Triangles indicate females, squares show males, and circles are juveniles.

3.7. Flow rate

The volume of fluid that flows between adjacent rows of aesthetascs per unit time is 2.36 (S.E. = 0.05, $n = 130$) times greater during the lateral motion of the flick than during the medial motion of the flick (Fig. 10). Flow rate between one pair of adjacent aesthetasc rows increases more than 20-fold as the animals increase in size from 8 to 55 mm rostrum–telson length. Flow rate between all aesthetasc rows on an antennule filament increases more than 200-fold as the animals grow over the same range of body sizes (Fig. 11). In both cases, the difference in flow rate between males and females is not statistically significant (Table 2).

3.8. Flicking frequency

Maximum flicking frequency increased from two to seven flicks per second as the total body length increased from 8 to 52 mm (Fig. 12).

4. Discussion

Odorant access to the aesthetascs on stomatopod olfactory antennules is affected by flow near the aesthetascs when the animals flick their antennules. We have used kinematic and morphological data to calculate estimates of the water flow between rows of aesthetascs of stomatopods as they grow from newly-settled juveniles to mature males and females. Such water flow should affect how these animals sample their chemical environments.

4.1. Flow through the aesthetasc array during a flick

The Re of the flow around the aesthetascs during the outward part of the flick is always greater than the Re of the flow around the aesthetascs during the return inward part of the flick. The mean ratio of outward Re to inward Re is 1.91 (SD = 0.03, $n = 130$). Both mathematical models (Cheer and Koehl, 1987; Koehl, 1995; 1996a, 1996b) and physical models (Hansen and Tiselius, 1992; Louden et al., 1994; Koehl, 1995) of flow between neighboring cylinders in an array suggest that the leakiness of an array of closely-spaced hairs (gap-to-diameter ratios of 10 or lower, as found in the spacing of rows of aesthetascs along stomatopod antennules) operating in the Re range of stomatopod aesthetascs (Re = 0.1–1.8) is very sensitive to changes in Re. This suggests that stomatopod antennules operate in a Re range that enhances the difference in leakiness between the fast outward part of the flick and the slower return. Thus, new water and any odorants it may bear should penetrate the aesthetasc array more during the leaky lateral motion than during the slower medial motion of a flick. One consequence of this difference in leakiness is that the water surrounding the aesthetascs at the end of a flick is different from the water surrounding them before the flick, even when the aesthetascs return to their original position. This mechanism has been suggested for the

antennules of spiny lobsters, which also show an asymmetry in aesthetasc Re during the downward versus upward portions of a flick (Goldman and Koehl, 1999).

Another consequence of the difference in aesthetasc Re between the outward and return parts of the flick is that the boundary layer around the aesthetascs is thinner during the outward motion than during the return motion. Hence the time needed for odorants to diffuse from newly-sampled water to the aesthetasc is less during the lateral movement than during the medial stroke. When flow rates through an array of setae are high and boundary layers are thin, the number of molecules captured per time by the setae is greater than when flow rates are low and boundary layers are thick (e.g., Shimeta and Jumars, 1991; Koehl, 1996a, 1996b). The shorter response time and higher capture rate when flow rate is high and boundary layers are thin suggests that changes in odor molecule concentration may be important cues under these conditions (Koehl, 1996a, 1996b). In contrast, when flow rates through an array of hairs are low, there is more time for molecules in the water being sampled to diffuse to hair surfaces. Under these conditions, a greater proportion of the molecules in the sample water are caught (e.g., Rubenstein and Koehl, 1977; Koehl, 1996a, 1996b), although response time may be long and capture rates low.

The difference in Re of the outward and inward parts of a stomatopod antennule flick suggest that the rapid outward motion removes ''old'' already-sampled water from the aesthetasc array and allows penetration of new odorant-bearing water close to aesthetasc surfaces, similar to the downstroke of a lobster antennule flick (e.g., Schmidt and Ache, 1979; Moore et al., 1991; Goldman and Koehl, 1999). Goldman and Koehl (1999) suggested that this difference in odorant access during different portions of the flick contributes to the ability of a flicking antennule to take discrete temporal and spatial samples of their chemical environment.

4.2. Scaling of antennules as stomatopods grow

Because stomatopod aesthetascs operate in a Re range in which flow rate through the aesthetasc array is very sensitive to changes in Re, the size (L in Eq. (1)) and speed (U in Eq. (1)) changes that occur as animals grow might affect antennule performance. The smallest stomatopods operate their antennules at aesthetasc Re values of 0.1–0.2, while large stomatopods operate at aesthetasc Re values between 1 and 2 (Fig. 8). Therefore, the aesthetascs of small stomatopods have relatively thick boundary layers, low leakiness, and little water flowing between adjacent rows, whereas those of large animals develop thin boundary layers, show high leakiness, and have proportionally more fluid flowing between the rows of aesthetascs (Figs. 9–11).

The differences in aesthetasc Re, leakiness, and flow rate of small and large stomatopods could have several functional consequences. The higher flow rate through the aesthetasc arrays of large stomatopods should enable them to shed ''old'' water from their antennules more quickly and completely than small animals can. Furthermore, the thinner boundary layers that form around the aesthetascs of large stomatopods should permit more rapid odorant diffusion to aesthetasc surfaces than for smaller animals. Thus, large animals should be more sensitive than small ones to changes in odorant concentration and should be able to take more temporally and spatially discrete samples

of their chemical environment when they flick. However, while the thick boundary layers surrounding the aesthetascs of small animals mean that odorant diffusion is slow, the reduced fluid flow may allow a greater proportion of odorant molecules to diffuse to the sensillum before they are swept away than for large animals.

4.3. Changes in stomatopod behavior and ecology with size and age

Several aspects of stomatopod life history suggest that the ecological requirements for smelling may change as stomatopods grow and mature. Since newly-settled *Gonodactylus* are not yet territorial, do not have social interactions that require recognition of individual conspecifics, and do not hunt motile prey (Caldwell et al., 1989), they may not rely heavily on smell at this stage. After animals grow to body lengths of 12–15 mm, they start to engage in contests over burrows in coral rubble (Caldwell et al., 1989). Furthermore, as the animals grow, the size and speed of their preferred prey (crabs, molluscs, worms) increases (Caldwell et al., 1989). *G. mutatus* begin breeding when they reach rostrum–telson lengths of 35–40 mm (Caldwell, pers. comm.). Assessing burrow inhabitants (for mate choice or habitat competition), burrow defense, and finding prey are likely to require rapid chemosensory sampling. The fact that social interactions and aggression, hunting of prey, and mating become increasingly important as stomatopods grow suggests that gathering olfactory information becomes more critical to stomatopods at the sizes at which their aesthetasc arrays become leakier (permitting greater odorant penetration) and the frequency of olfactory flicking increases.

4.4. Comparison with antennules of other crustaceans

The kinematics and the morphometrics of the antennules of the spiny lobster, *Panulirus argus* (Gleeson et al., 1993; Goldman and Koehl, 1999), and the American lobster, *Homarus americanus* (Moore et al., 1991; Best, 1995) have been analyzed and can be compared with those of the stomatopod, *G. mutatus*. These two species of lobsters bear their aesthetascs on the terminal portion of the lateral branch of each antennule. *P. argus* aesthetascs operate at a Re of 2 on the downstroke and at a Re of 0.5 during the upstroke (Goldman and Koehl, 1999), while the aesthetascs of *H. americanus* operate at Re values of 3–4 (Moore et al., 1991; Best, pers. comm.). In contrast to stomatopods, lobsters maintain the same aesthetasc Re as they grow (Best, 1995; Goldman and Koehl, 1999). Best (1995), who observed that aesthetasc Re was conserved over a 20-fold increase in body length, suggested that the nature of the flow around the sensory hairs and antennules may be very important to the processing of information during chemoreception. Goldman and Koehl (1999) suggested that lobsters maintain the Re of their aesthetascs as they grow in a range where the difference in leakiness is enhanced between the rapid downstroke and the slower upstroke. Because aesthetasc kinematics have only been quantified for a few species, it is not clear whether maintaining Re (as lobsters do) or increasing Re (as stomatopods do) as animals grow is more prevalent.

5. Conclusion

Our study of the flicking kinematics and the morphology of the olfactory antennules of the stomatopods *Gonodactylus mutatus* revealed that their olfactory setae, the aesthetascs, operate at a range of Reynolds numbers where the leakiness of an array is very sensitive to changes in speed and setal dimensions. As a consequence the flow rate of water through the array of aesthetascs is greater during the rapid lateral motion of an antennule flick than during the following slower motion. This leakiness asymmetry suggests that ''old'' water that has already been sampled is shed from the aesthetascs during the rapid lateral motion while ''new'' water and the odorants it carries penetrate the array, and then are retained during the slower medial motion. As stomatopods grow and mature, the Re of their aesthetascs increases nine-fold, aesthetasc leakiness doubles, and flow rate through the aesthetasc arrays increases by a factor of 200. These changes in antennule hydrodynamics, which should increase the rate at which odorant molecules arrive at aesthetasc surfaces and should improve the sensitivity of the antennules to changes in odorant concentration from one flick to the next, accompany behavioral and ecological changes that the stomatopods undergo as they grow. As these animals grow in size and mature, their increasing ability to acquire rapid, accurate olfactory information is undoubtedly important as they step up their efforts to hunt animal prey, to compete for burrows, and to seek mates.

Acknowledgements

We are grateful to R. Caldwell for his invaluable advice and support. We thank C. Fiedler and the staff at Hawaii Institute for Marine Biology where the animals were collected, P. Sicurello for instruction in SEM, K. Vetter for assistance in the field, the biomechanics group at U.C. Berkeley, F. Grasso and H. Trapido-Rosenthal for instructive feedback. These experiments were funded by ONR grant N00014-96-1-0594 to M.K.

References

Ache, B.W., 1982. Chemoreception and thermoreception. In: Atwood, H.L., Standeman, D.C. (Eds.), The Biology of Crustacea, Vol. 3, Academic Press, New York, pp. 369–393.

Atema, J., Voigt, R., 1995. Behavior and sensory biology. In: Factor, J.R. (Ed.), Biology of the Lobster *Homarus americanus*, Academic Press, San Diego, CA, pp. 313–348.

Best, B., 1995. Scaling and flow dynamics of crustacean antennules: What's flicking all about? Am. Zool. 35, 53A.

Caldwell, R.L., 1979. Cavity occupation and defensive behaviour in the stomatopod *Gonodactylus festae*: evidence for chemically mediated individual recognition. Anim. Behav. 27, 194–201.

Caldwell, R.L., 1985. A test of individual recognition in the stomatopod *Gonodactylus festae*. Anim. Behav. 33, 101–106.

Caldwell, R.L., 1987. Assessment strategies in stomatopods. Bull. Mar. Sci. 41, 135–150.

Caldwell, R.L., Roderick, G.K., Shuster, S.M., 1989. Studies of predation by *Gonodactylus bredini*. In: Ferrero, E.A. (Ed.), Biology of Stomatopods. Collana UZI, Selected Symposia and Monographs, Mucchi Editore, Modena, pp. 117–131.

Cheer, A.Y.L., Koehl, M.A.R., 1987. Paddles and rakes: fluid flow through bristled appendages of small organisms. J. Theor. Biol. 129, 17–39.

Fuller, W.A., 1987. Measurement Error Models, John Wiley and Sons, New York.

Gleeson, R.A., 1982. Morphological and behavioral identification of the sensory structures mediating pheromone reception reception in the blue crab, *Callinectes sapidus*. Biol. Bull. 163, 162–171.

Gleeson, R.A., Carr, W.E.S., Trapido-Rosenthal, H.G., 1993. Morphological characteristics facilitating stimulus access and removal in the olfactory organ of the spiny lobster, *Panulirus argus*: insight from the design. Chem. Senses 18, 67–75.

Goldman, J., Koehl, M.A.R., 1999. Fluid dynamic design of lobster olfactory organs: high-speed kinematic analysis of antennule flicking by *Panulirus argus*. Chem. Senses submitted for publication.

Grünert, U., Ache, B.W., 1988. Ultrastructure of the aesthetasc (olfactory) sensilla of the spiny lobster, *Panulirus argus*. Cell Tissue Res. 251, 95–103.

Hallberg, E., Johansson, K.U.I., Elofsson, R., 1992. The aesthetasc concept: structural variations of putative olfactory receptor cell complexes in Crustacea. Micros. Res. Techn. 22, 325–335.

Hansen, B., Tiselius, P., 1992. Flow through feeding structures of suspension feeding zooplankton: a physical model approach. J. Plankton Res. 14, 821–834.

Heimann, P., 1984. Fine structure and molting of the aesthetasc sense organs on the antennules of the isopod, *Asellus aquaticus* (Crustacea). Cell Tissue Res. 235, 117–128.

Johnson, A.S., Koehl, M.A.R., 1994. Maintenance of dynamic strain similarity and environmental stress factor in different flow habitats: thallus allometry and material properties of a giant kelp. J. Exp. Biol. 195, 381–410.

Koehl, M.A.R., 1995. Fluid flow through hair-bearing appendages: feeding, smelling and swimming at low and intermediate Reynolds numbers. In: Ellington, C.P., Pedley, T.J. (Eds.), Soc. Exp. Biol. Symp., Biological Fluid Dynamics, Vol. 49, pp. 157–182.

Koehl, M.A.R., 1996a. Small-scale fluid dynamics of olfactory antennae. Mar. Fresh. Behav. Physiol. 27, 127–141.

Koehl, M.A.R., 1996b. When does morphology matter? Annu. Rev. Ecol. Syst. 27, 501–542.

LaBarbara, M., 1989. Analyzing body size as a factor in ecology and evolution. Ann. Rev. Ecol. Syst. 20, 97–117.

Louden, C., Best, B., Koehl, M.A.R., 1994. When does motion relative to neighboring surfaces alter the flow through arrays of hairs? J. Exp. Biol. 193, 233–254.

Moore, P.A., Atema, J., Gerhardt, G.A., 1991. Fluid dynamics and microscale chemical movement in the chemosensory appendages of the lobster, *Homarus americanus*. Chem. Senses 16, 663–674.

Rubenstein, D.I., Koehl, M.A.R., 1977. The mechanisms of filter feeding: some theoretical considerations. Am. Nat. 111, 981–994.

Schlichting, H., 1979. Boundary-Layer Theory, 7th ed., McGraw-Hill, London.

Schmidt, B.C., Ache, B.W., 1979. Olfaction: responses of a decapod crustacean are enhanced by flicking. Science 205, 204–206.

Shimeta, J., Jumars, P., 1991. Physical mechanisms and rates of particle capture by suspension feeders. Oceanogr. Mar. Biol. Ann. Rev. 29, 191–257.

Slifer, E.H., 1960. A rapid and sensitive method for identifying permeable areas in the body wall of insects. Ent. News 71, 179–182.

Sokal, R.R., Rohlf, F.J., 1995. Biometry, 3rd ed., W.H. Freeman.

Vogel, S., 1994. Life in Moving Fluids, 2nd ed., Princeton University Press, Princeton, NJ.

Zimmer-Faust, R.K., 1989. The relationship between chemoreception and foraging behavior in crustaceans. Limnol. Oceanogr. 34, 1364–1374.